Empirical formula for the vibration reduction index of junctions with different coplanar walls

C. Crispin[1], C. Mertens[1], A. Dijckmans[1]
[1] Belgian Building Research Institute, Acoustic division
Rue du Lombart 42, B-1000, Brussels, Belgium
e-mail: **charlotte.crispin@bbri.be**

Abstract

The vibration reduction index K_{ij} is a normalized quantity related to the vibrational power transmission over a structural junction in a building. Its measured or predicted value is used in prediction models in order to determine the contribution of the flanking transmission in the global sound transmission between rooms.

The predicted values provided in the standard ISO 12354-1 concern mainly rather simple junctions. This article suggests new engineering approximations for junctions of which the coplanar walls are different. These types of junction are roughly addressed in the standard. The empirical formulas, easy to use, are derived from a large number of numerical simulations and some measurements.

1 Introduction

The vibration reduction index, $K_{ij,}$ expresses the vibrational power transmission over a junction between two physically connected building elements in function of the frequency. The K_{ij} can be evaluated by measurement according to the standard ISO 10848 [1] or by prediction formulas presented in the annex E of the standard ISO 12354-1[2].

This article studies the K_{ij} for particular junctions named, here, rigid mixed cross-junctions that means cross-junctions composed of two different coplanar walls. The annex J of the standard 12354 proposes a rather simplistic interpretation to address these particular junctions: It proposes to replace the two different coplanar walls by two identical walls whose surface mass is the average of the surface mass of these walls (Figure 1). This article therefore supplies more relevant formulas which are derived from numerical simulations based on the finite element method (FEM, software Actran 15), statistical energy analysis (SEA) and the wave based method (WBM) [5].

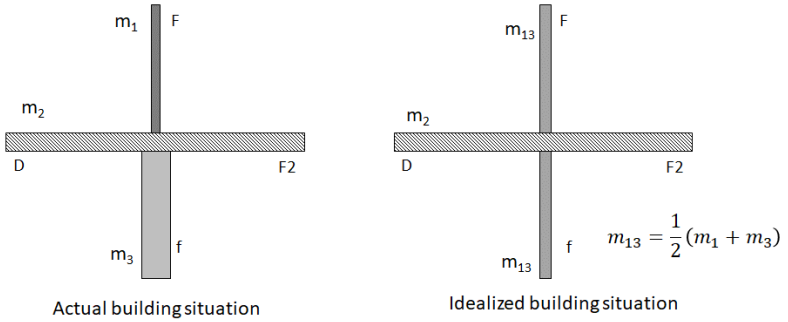

Figure 1: Interpretation for cross-junction with more than 2 element types according to annex J of the standard 12354-1 [2]

2 The vibration reduction index K_{ij} and its single-values

According to the measurement method (ISO 10848 [1]), the K_{ij} is estimated by the average of the velocity level differences $D_{v,ij}$ and $D_{v,ji}$ normalized to the junction length and the equivalent sound absorption length according to following formula:

$$K_{ij} = \overline{D}_{v,ij} + 10\lg\frac{l_{ij}}{\sqrt{a_i a_j}} \quad [\text{dB}] \tag{1}$$

$\overline{D}_{v,ij}$ is the direction averaged velocity level difference. It is obtained from the mean value of the velocity level differences $D_{v,ij}$ (when wall i is excited) and $D_{v,ji}$ (when the j is excited). It is expressed in decibels:

$$\overline{D}_{v,ij} = \frac{1}{2}\left(D_{v,ij} + D_{v,ji}\right) \quad [\text{dB}] \tag{2}$$

a_i (a_j, resp.) is the equivalent absorption length of wall i (wall j, resp.). It is expressed in meters.

$$a_i = \frac{2.2\pi^2 S_i}{c_0 T_{si}}\sqrt{\frac{f_{ref}}{f}} \quad [\text{m}] \tag{3}$$

where, S_i is the surface area of wall i [m²];
$T_{s,i}$ is the structural reverberation time of wall i [s];
c_0 is the speed of sound in air [m/s];
f is the current frequency [Hz];
f_{ref} is the reference frequency [f_{ref} = 1000 Hz].

The measured K_{ij} can be expressed by a single value $\overline{K_{ij}}$ which is the arithmetic average of K_{ij} within the frequency range 200 Hz- 1250 Hz.

Annex E of the standard ISO 12354-1[2], for its part, proposes two methods to predict the K_{ij} for heavy structures. The first method considers that the K_{ij} is frequency-independent and gives a constant value for all frequencies. The empirical data are deduced from standardized measurements, theory or both and are expressed in terms of the ratio of the surface masses of the elements in the junction.

The data of the second method come from simulations [3]. These data are more difficult to use but more traceable. Futhermore, the K_{ij} is given in three different frequency ranges because in practice, it is shown that the K_{ij} is not really frequency independent:

- $K_{ij,low}$ is the arithmetic average of the one-third octave band values from 50 Hz to 200 Hz;
- $K_{ij,mid}$ is the arithmetic average of the one-third octave band values from 250 Hz to 1000 Hz;
- $K_{ij,high}$ is the arithmetic average of the one-third octave band values from 1250 Hz to 5000 Hz.

According to this method, the K_{ij} is determined by the characteristic moment-impedance, named the PC ratio (see section 5).

To be consistent with this annex the new prediction formulas dedicated to rigid mixed cross-junctions are given for the two approaches in sections 4 and 5, respectively.

3 Numerical simulations

Details of the FEM, SEA and WBM models developed to predict the vibration transmission across rigid plate junctions can be found in previous publications [4, 5, 13, 14]. All the models assume homogeneous, acoustically thin plates and unpinned junction lines. They take into account the finite dimensions of the plates and include both in-plane and bending wave vibration. The main difference between WBM and FEM are the plate boundary conditions: while the FEM model incorporates free plate boundary conditions, the WBM assumes simply supported plates. The frequency-dependent loss factor needed to evaluate the damping of the walls is set equal to $1/\sqrt{f}$. The dimensions of the floor F1 (and F2) used in the WBM and SEA models are 5m x 4m. The dimensions of the wall Wh (and Wl) used in the WBM and SEA models are 3.5 m x 4 m. For the FEM simulations, the floor dimensions are 4 m x 2.74 m and the wall dimensions 4 m x 2.38 m.

The material properties used in the simulations are given in tables 1 and 2.

Surface mass of the concrete floor $m'_{F1\text{-}F2}$ [kg/m²]	Surface mass of the heavy wall m'_{Wh} [kg/m²]	Surface mass of the 10 cm lightweight wall m'_{Wl} [kg/m²]	Numerical simulation used to study these combinations
276 (h=12 cm, ρ=2300kg/m³)	230 (h=10 cm, ρ=2300kg/m³)	40, 80, 140, 175, 180, 200, 220, 230	WBM, SEA
276 (h=12 cm, ρ=2300kg/m³)	345 (h=15 cm, ρ=2300kg/m³)	40, 80, 140, 175, 180, 200, 220, 230, 276 (12 cm), 345 (15 cm)	WBM, SEA
460 (h=20 cm, ρ=2300kg/m³)	230 (h=10 cm, ρ=2300kg/m³)	40, 80, 140, 175, 180, 200, 220, 230	WBM, SEA, FEM
460 (h=20 cm, ρ=2300kg/m³)	345 (h=15 cm, ρ=2300kg/m³)	40, 80, 140, 175, 180, 200, 220, 230, 276 (12 cm), 345 (15 cm)	WBM, SEA
644 (h=28 cm, ρ=2300kg/m³)	230 (h=10 cm, ρ=2300kg/m³)	40, 80, 140, 175, 180, 200, 220, 230	WBM, SEA
644 (h=28 cm, ρ=2300kg/m³)	345 (h=15 cm, ρ=2300kg/m³)	40, 80, 140, 175, 180, 200, 220, 230, 276 (12 cm), 345 (15 cm)	WBM, SEA

Table 1: Studied combinations for the rigid mixed cross-junctions

The Poisson's ratio is 0.2 and the Young's modulus in function of the density is given in table 2.

ρ [kg/m³]	**E_{dyn} [N/m²]**
400	1.32×10^9
800	2.51×10^9
1400	6.56×10^9
1750	1.22×10^{10}
1800	1.24×10^{10}
2000	1.71×10^{10}
2200	2.36×10^{10}
2300	2.6×10^{10}

Table 2: Young's modulus used for the numerical simulations

4 Empirical formula for K_{ij} in function of the surface mass ratio

4.1 Path F1-F2

For this path, it is expected that the vibration reduction index of the mixed junction is between the value of the rigid T-junction when the surface mass of the lightweight wall tends towards zero, $K_{F1\text{-}F2,T,Wh,}$ and the value of the rigid cross-junction when the surface mass of the lightweight wall is equal to the heavy wall, $K_{F1\text{-}F2,X,Wh}$. The expected form of the K_{ij} for the mixed junction is then:

$$K_{F1-F2,mixed} = p * K_{F1-F2,X,Wh} + (1-p) * K_{F1-F2,T,Wh} \quad (4)$$

where p is the weight factor to evaluate.

To this end, a large number of numerical simulations was carried out. The $K_{F1\text{-}F2,mixed}$ were determined numerically for the combinations given at table 1 with the corresponding $K_{F1\text{-}F2,X,Wh}$ and $K_{F1\text{-}F2,T,Wh}$. For each combination, the factor p was calculated with Eqn. (4). By plotting the data on a chart, the linear relationship between p and the ratio of the surface masses of the two walls is well observed (Figure 2). While ensuring that p equals 1 for m'_{wl} equals m'_{wh} and that p equals 0 for m'_{wl} equals 0, it can be approximated by:

$$p = \left(\frac{m'_{Wl}}{m'_{Wh}}\right) \quad (5)$$

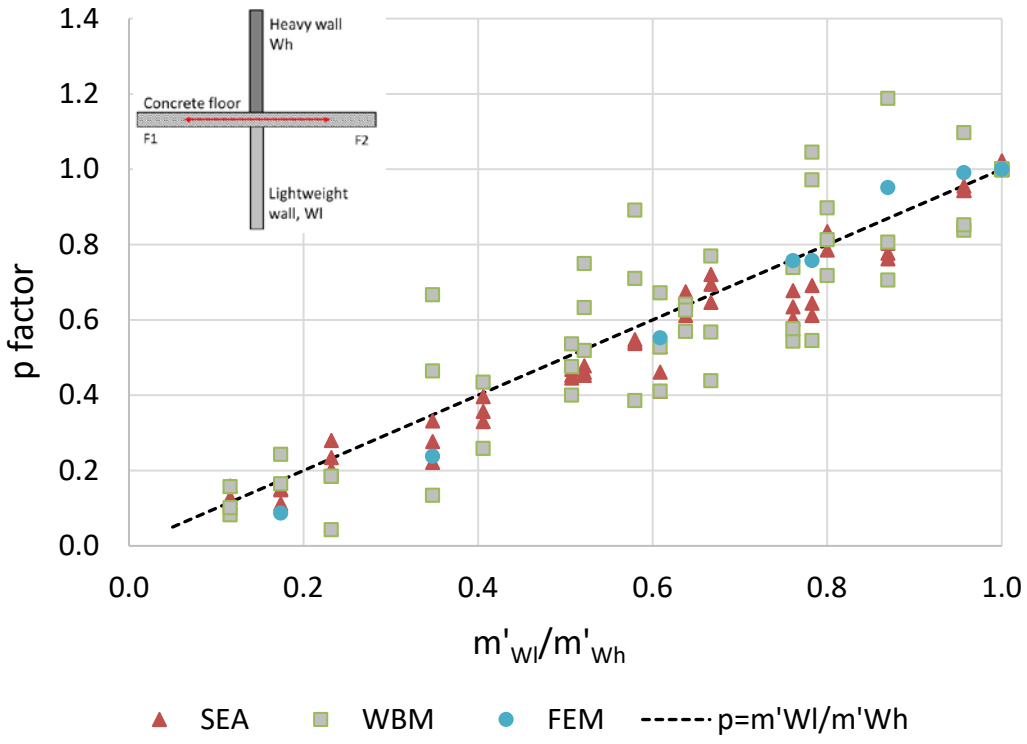

Figure 2: Weight factor p obtained by simulations for the transmission path F1-F2

The coefficient of determination, R^2, for this trendline is 0.99 for FEM data, 0.95 for SEA data and 0.77 for WBM data. The WBM data are more scattered than the SEA data due to the significant influence of the

plate modal behavior in a broad frequency range [9,14]. While the FEM also incorporates the modal behavior, the variation seen in the eight test cases is smaller.

The new prediction according to Eqn. (4) is more accurate than the prediction proposed in annex J of the standard ISO 12354-1 where the mixed junction is replaced by an idealized junction (see figure 1). The accuracy of Eqn. (4) and the ISO 12354-1 prediction was evaluated on some SEA simulations (Figure 3a and 3b).

These figures present the calculation error obtained with the new prediction (the absolute difference between the expected values and the new prediction) and with the 12354 prediction (the absolute difference between the expected values and the 12354 prediction) for different surface mass ratio's between the walls. All data (expected values, new prediction values and 12354 values) come from SEA simulations.

For a floor having a surface mass higher than the heavy wall, an error close to 2 dB can be observed with the 12354 prediction when the surface mass ratio is low. With the new prediction, this error falls to approximately 1 dB.

For the other case ($m'_{F1}<m'_{Wh}$) the error is close to zero with the new prediction. The calculations errors obtained with the 12354 prediction is 1.2 dB for m'_{Wl}/m'_{Wh} equal to 0.12. As expected, the larger the difference in surface mass of the walls is, the larger the calculation errors obtained with the 12354 prediction is.

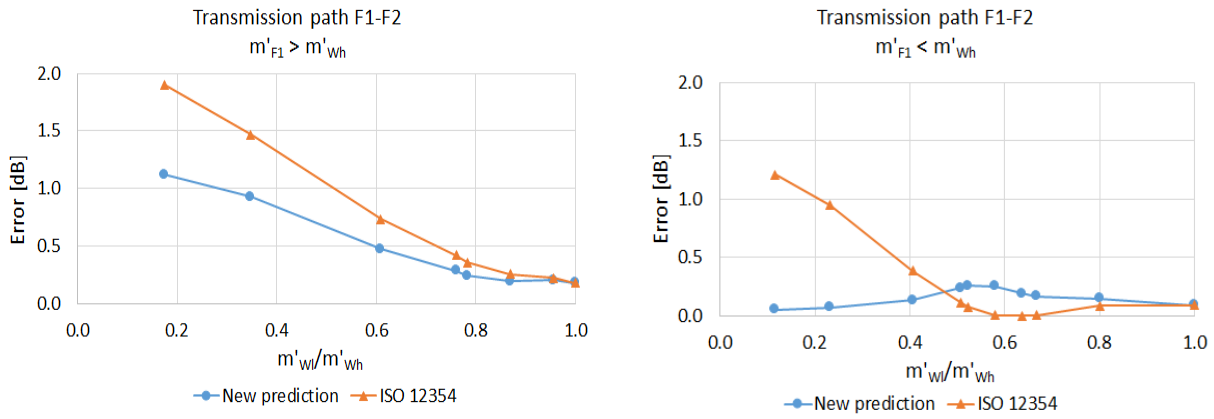

(a) (b)

Figures 3a and 3b: Transmission path F1-F2: Comparison between the calculation error [dB] of the new prediction and of the 12354 prediction obtained by SEA simulations in function of the surface mass ratio's between the walls. (a) for $m'_{F1}> m'_{Wh}$ and (b) for $m'_{F1}< m'_{Wh}$

4.2 Path Wh-Wl

This transmission path crosses the two coplanar walls with different properties. In this case, the following equation can be expected:

$$K_{Wh-Wl,mixed} = p * K_{Wh-Wl,X,Wm} \quad (6)$$

Where $K_{Wh\text{-}Wl,X,Wm}$ is the vibration reduction index of the simple rigid cross-junction of which the surface mass of the coplanar walls is the average of the surface mass of the walls Wh and Wl. As before, the $K_{Wh\text{-}Wl,mixed}$ of different combinations and the corresponding $K_{Wh\text{-}Wl,X,Wm}$ were obtained from the three numerical methods from which the p factor could be calculated. Figure 4 presents this factor in function of the ratio of the surface masses of the two walls.

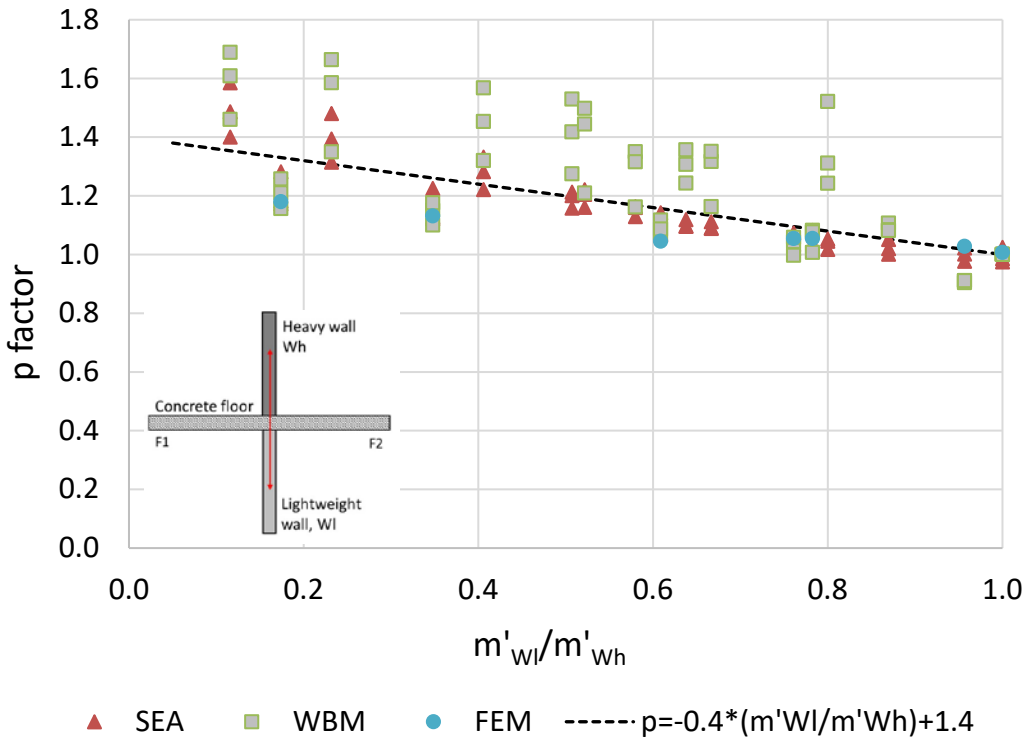

Figure 4: Weight factor *p* obtained by simulations for the transmission path Wh-Wl

Again, the WBM data are more scattered than the SEA data. The FEM data for the 10cm concrete heavy wall agree well with the WBM data. The WBM data for the 15cm concrete heavy wall are higher than the SEA data. The slope given by the FEM data is the lowest. While ensuring that *p* equals 1 for m'_{Wl} equals m'_{Wh}, the best trendline for all data is given by:

$$p = -0.4 * \left(\frac{m'_{Wl}}{m'_{Wh}}\right) + 1.4 \tag{7}$$

The coefficient of determination, R^2, for the SEA data is 0.77, for the FEM data, 0.92 and for the WBM, 0.48. As before, the calculation errors of the new prediction and of the 12354 prediction were evaluated by SEA simulations (Figures 5a and 5b).

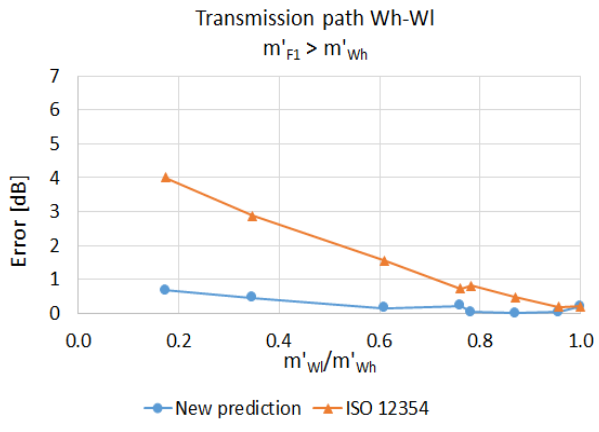

(a)

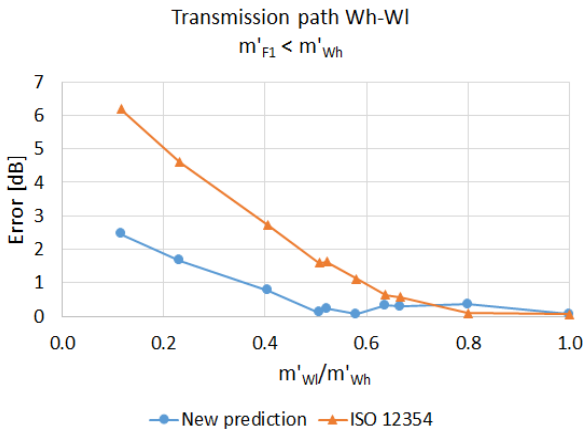

(b)

Figures 5a and 5b: Transmission path Wh-Wl : Comparison between the calculation error [dB] of the new prediction and of the 12354 prediction obtained by SEA simulations in function of the surface mass ratio's between the walls. (a) for $m'_{F1} > m'_{Wh}$ and (b) for $m'_{F1} < m'_{Wh}$

For $m'_{F1} > m'_{Wh}$, an error of 4 dB can be reached for a low surface mass ratio with the 12354 prediction. This error decreases when the surface mass ratio tends towards 1. The error of the new prediction is lower than 1 dB. For the case $m'_{F1} < m'_{Wh}$, the calculation errors obtained with the 12354 prediction can be higher than 6 dB, while the maximum error for the new prediction is 2.5 dB.

4.3 Path F1-Wh

For this transmission around the corner and involving the heaviest wall (Figure 6), it is expected that the $K_{F1\text{-}Wh,mixed}$ will be between two limit values: the value of the rigid T-junction , $K_{F1\text{-}Wh,T,Wh}$, when the surface mass of the lightweight wall tends towards zero, and the value of the rigid cross-junction, $K_{F1\text{-}Wh,X,Wh}$, when the surface mass of the lightweight wall is equal to the heavy wall:

$$K_{F1-Wh,mixed} = p * K_{F1-Wh,X,Wh} + (1-p) * K_{F1-Wh,T,Wh} \quad (8)$$

The weight factors p were calculated from several $K_{F1\text{-}Wh,mixed}$, $K_{F1\text{-}Wh,X,Wh}$ and $K_{F1\text{-}Wh,T,Wh}$ obtained by the three numerical simulations. The results are presented in figure 6 in function of the ratio of the surface masses of the walls W_l and W_h. The WBM method gives again widely scattered points due to the different modal behavior of the different junctions modeled. The best selected trendline is a polynomial relationship:

$$p = 0.4 * \left(\frac{m'_{Wl}}{m'_{Wh}}\right)^2 + 0.6\left(\frac{m'_{Wl}}{m'_{Wh}}\right) \quad (9)$$

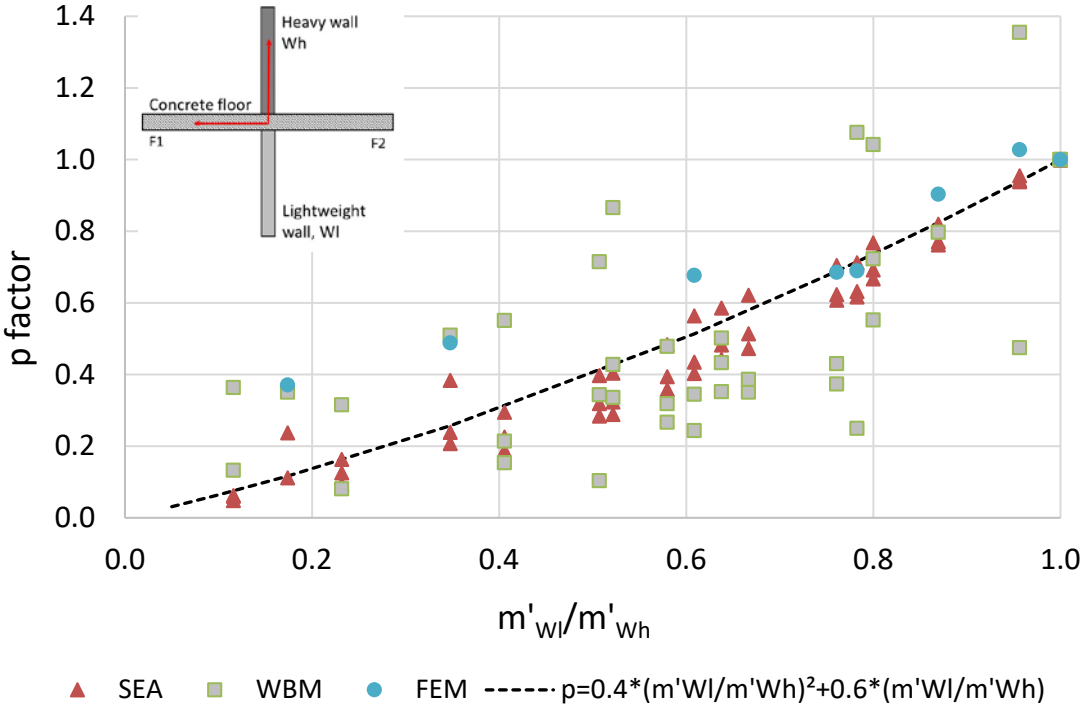

Figure 6: Weight factor p factor obtained by simulations for the transmission path F1-Wh

The coefficient of determination, R^2, for the SEA data is 0.96, for the FEM data, 0.93 and for the WBM, 0.55.

Figures 7a and 7b confirm that this new proposition is more accurate than the K_{ij} obtained by the 12354 prediction which uses the mean of the walls. The calculation errors obtained by the 12354 prediction increases significantly when the contrast between the surface masses increases. For example, a deviation of ± 4 dB is observed around a surface mass ratio of 0.2. The error for the new prediction is smaller than 1 dB.

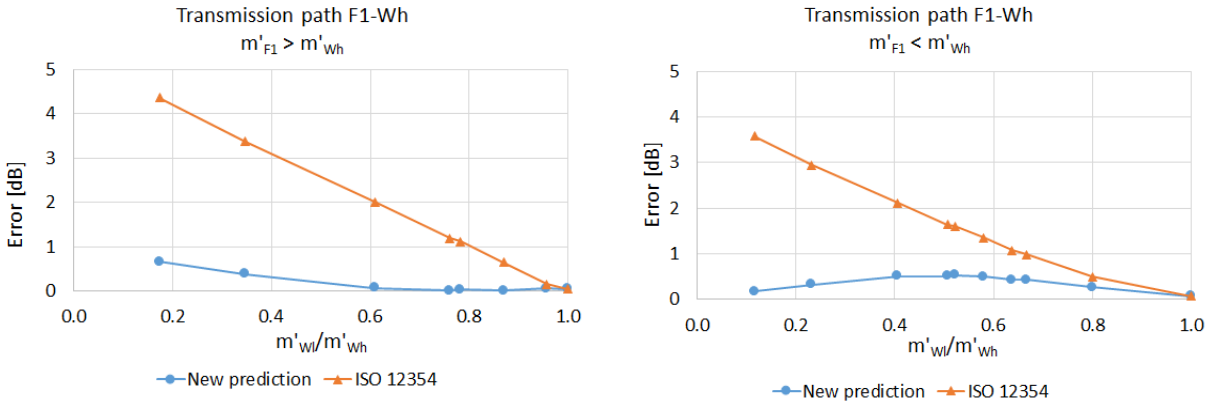

(a) (b)

Figures 7a and 7b: Transmission path F1-Wh : Comparison between the calculation error [dB] of the new prediction and of the 12354 prediction obtained by SEA simulations in function of the surface mass ratio's between the walls. (a) for $m'_{F1} > m'_{Wh}$ and (b) for $m'_{F1} < m'_{Wh}$

4.4 Path F1-Wl

In this case, the $K_{F1\text{-}Wl,mixed}$ is calculated from the $K_{F1\text{-}Wl,X,Wl}$ which represents the vibration reduction index of the rigid cross-junction of which the coplanar walls are identical and composed of the lightest walls W_l.

$$K_{F1-Wl,mixed} = p * K_{F1-Wl,X,Wl} \quad (10)$$

The p factors obtained with the numerical simulations are presented in figure 8. While the FEM method gives a slope close to zero, the WBM and SEA simulations follow the selected trendline (ensuring that p=1 for $m'_{Wl}=m'_{Wh}$), given by:

$$p = -0.4 * \left(\frac{m'_{Wl}}{m'_{Wh}}\right) + 1.4 \quad (11)$$

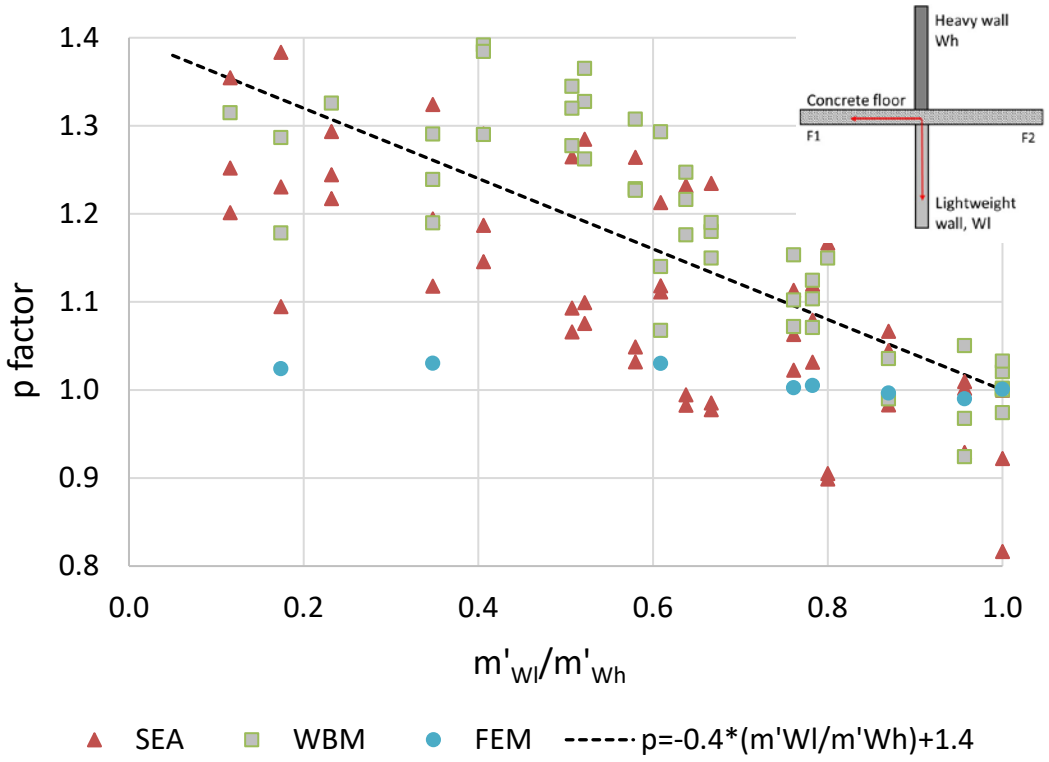

Figure 8: Weight factor p factor obtained by simulations for the transmission path F1-Wl

The coefficient of determination, R^2, for the SEA data is 0.75, for the FEM data, 0.70 and for the WBM, 0.74 giving mitigated results but nevertheless gives, according to some SEA results (figures 9), a quite good prediction compared to the prediction which uses the mean of the walls. For example, an error higher than 5 dB is already observed between the actual mixed junction value and the 12354 prediction value for a surface mass ratio around 0.5. This error can increase if the surface mass ratio tends towards 0. The error is smaller than 1 dB with the new prediction and remains relatively constant in terms of the surface mass ratio.

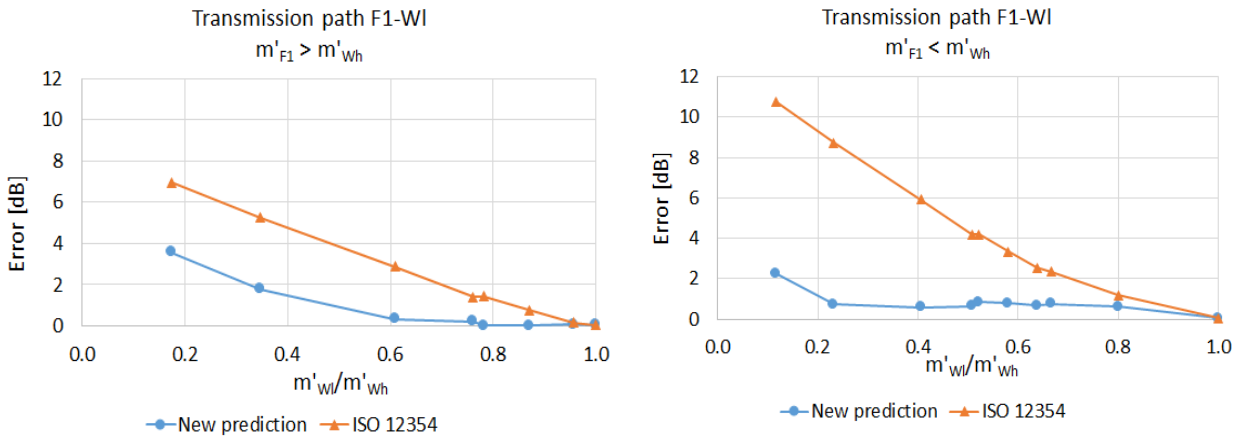

(a) (b)

Figures 9a and 9b: Transmission path F1-Wl : Comparison between the calculation error [dB] of the new prediction and of the 12354 prediction obtained by SEA simulations in function of the surface mass ratio's between the walls. (a) for $m'_{F1} > m'_{Wh}$ and (b) for $m'_{F1} < m'_{Wh}$

5 Empirical formula for K_{ij} in function of the characteristic moment-impedances ratio

In the new version of the standard ISO 12354-1 [1], more accurate and traceable formulas are now available. These formulas come from numerical simulations and concern, for the time, only rigid L-, T- and X-junctions of homogeneous, isotropic plates. We propose here to extend these formulas to rigid cross-mixed junctions in the same way.

In this case, the prediction of K_{ij} must be given in three different frequency ranges in order to take into account the effect of in-plane waves as well as bending waves: a low-frequency range (50 Hz to 200 Hz), a mid-frequency range (250 Hz to 1k Hz) and a high-frequency range (1.25 kHz to 5 kHz). Furthermore, the K_{ij} is expressed as a function of the ratio of the characteristic moment-impedances (PC ratio) instead of the surface masses [3, 4]. That is why the weight factor p mentioned above will be in this case a function of this ratio too.

$$PC\ ratio = \sqrt[4]{\frac{m'_{\perp i}B^3_{\perp i}}{m'_i B^3_i}} = \left(\frac{\rho_{\perp i}}{\rho_i}\right)^{1/4}\left(\frac{h_{\perp i}}{h_i}\right)^{5/2}\left(\frac{E_{\perp i}}{E_i}\right)^{3/4} \tag{12}$$

Figures 10a to 10d present the $K_{ij,low}$, $K_{ij,mid}$ and $K_{ij,high}$ per transmission path for the three different frequency ranges. On each graph, the distinction between the three numerical simulations is not visible anymore but the three ranges are highlighted as well the selected trendline for p.

The results in the low frequency range are very scattered. This is not surprising because in low frequency the determination of the single value is less accurate due to the low number of modes. The dispersion of the results increases as the PC ratio decreases.

It seems that a single trendline could be appropriate for the three frequency ranges. It is advantageous to avoid the risk of errors when calculating the predictions.

The coefficients of the determination are not very high, especially for the low frequency range but these propositions of prediction offer better results than the ones reached by the predictions which use the mean of the PC ratio of the walls.

In conclusion, the weight factor p for the transmission path F1-F2 (Figure 10a) is given by:

$$p = -0.9 * \left(\sqrt[4]{\frac{m'_{Wl}B^3_{Wl}}{m'_{Wh}B^3_{Wh}}}\right)^2 + 1.9 * \left(\sqrt[4]{\frac{m'_{Wl}B^3_{Wl}}{m'_{Wh}B^3_{Wh}}}\right) \tag{13}$$

This factor is applied in Eqn. (4) where the $K_{F1\text{-}F2,mixed}$, $K_{F1\text{-}F2,X,Wh}$ and $K_{F1\text{-}F2,T,Wh}$ are replaced by the corresponding values at low (mid and high, resp.) frequencies for a prediction in the low (mid and high, resp.) frequency range.

For the transmission path Wh-Wl (Figure 10c), the weight factor p that has to be applied in Eqn. (6) is:

$$p = 0.8 * \left(\sqrt[4]{\frac{m'_{Wl}B^3_{Wl}}{m'_{Wh}B^3_{Wh}}}\right)^2 - 1.5 * \left(\sqrt[4]{\frac{m'_{Wl}B^3_{Wl}}{m'_{Wh}B^3_{Wh}}}\right) + 1.7 \tag{14}$$

For the transmission path F1-Wh (Figure 10b), the weight factor p that has to be applied in Eqn. (8) is:

$$p = -0.5 * \left(\sqrt[4]{\frac{m'_{Wl}B^3_{Wl}}{m'_{Wh}B^3_{Wh}}}\right)^2 + 1.5 * \left(\sqrt[4]{\frac{m'_{Wl}B^3_{Wl}}{m'_{Wh}B^3_{Wh}}}\right) \tag{15}$$

For the transmission path F1-Wl (Figure 10d), the weight factor p that has to be applied in Eqn. (10) is:

$$p = -0.15 * \left(\sqrt[4]{\frac{m'_{Wl}B^3_{Wl}}{m'_{Wh}B^3_{Wh}}}\right) + 1.15 \tag{16}$$

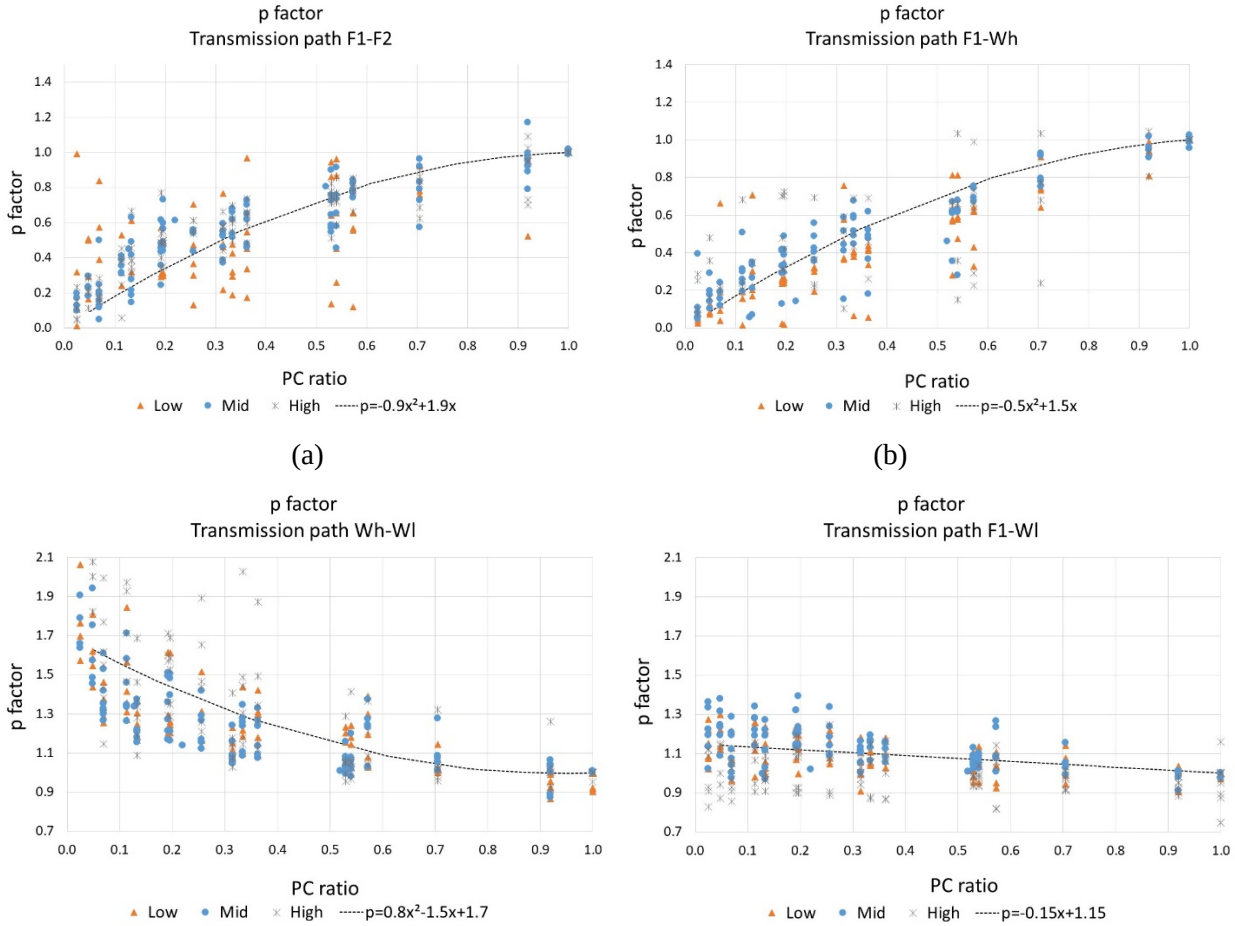

Figure 10: Weight factor *p* in function of the PC ratio obtained by simulations for (a) the transmission path F1-F2 (b) the transmission path F1-Wh (c) the transmission path Wh-Wl (d) the transmission path F1-Wl

6 Experimental validation

6.1 Test constructions and measurement procedure

The assessment of the vibration transmission reduction through rigid mixed cross-junctions was carried out on a junction where the floor, F1-F2 (100 mm), was composed of a reinforced concrete plate, the heavy wall was composed of solid concrete blocks (90 mm) and the lightweight wall was composed of cellular concrete blocks (70 mm). The experimental results have been obtained according to the specifications of the standard 10848 but on a half scaled test bench (Figure 11) [5, 6, 7].

Figure 11: pictures of the measurement setup

The properties of the walls are given at table 3.

Material	Thickness [mm]	Density [kg/m³]	Surface mass [kg/m²]	c_L [m/s]	fc [Hz]	Edyn [N/m²]
reinforced concrete	100	2300	230	3400	190	2.60E+10
Concrete blocks	90	2300	207	3400	210	2.60E+10
Cellular concrete blocks	70	666	47	1650	563	1.74E+09

Table 3: properties of the materials

6.2 Results

The idea, here, is:

- To calculate the prediction of rigid mixed cross-junction on the basis of the new weight factor *p* applied on the K_{ij} (or $K_{ij,low}$, $K_{ij,mid}$, $K_{ij,high}$) proposed in the standard ISO 12354-1 [1];
- To calculate the prediction according to annex J of the standard 12354 where the surface mass is the average of the walls Wh and Wl (or the average of the characteristic moment impedance);
- To compare these results with the measured values.

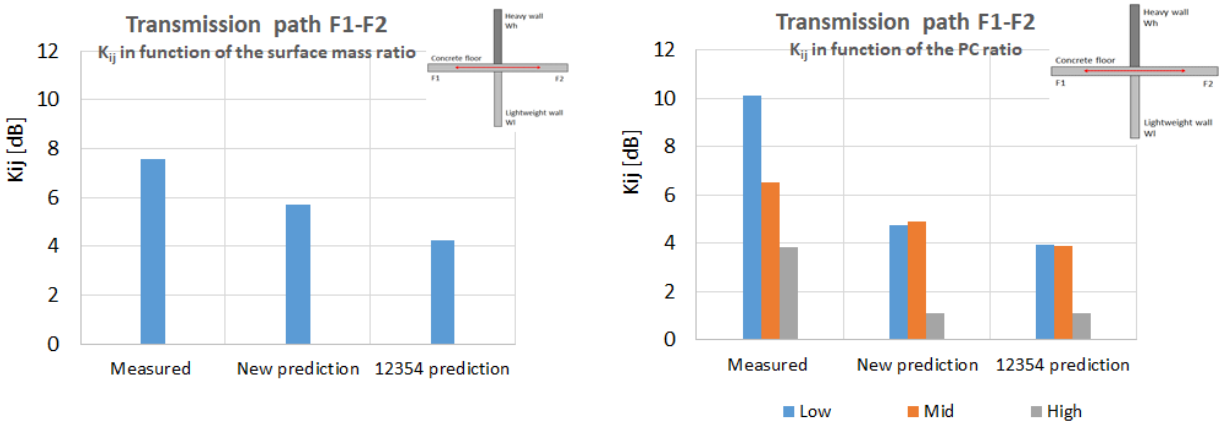

(a) (b)

Figure 12: Path F1-F2: Comparison between the measured results, the new prediction results and the prediction results obtained according to the annex J of the standard 12354. (a) for K_{ij} expressed in terms of the surface mass ratio, (b) for K_{ij} expressed in terms of PC ratio.

Overall, we find, for the path F1-F2 (figures 12a and 12b) an improvement of the new prediction with the use of the weight factor p. The predictions are still lower than the measured results. This is due to the fact that the initial prediction formulas of the standard 12354-1 underestimate the $\overline{K_{ij}}$ for this path. The measured $K_{ij,low}$ is unduly high because there is a lack of modes in this frequency range.

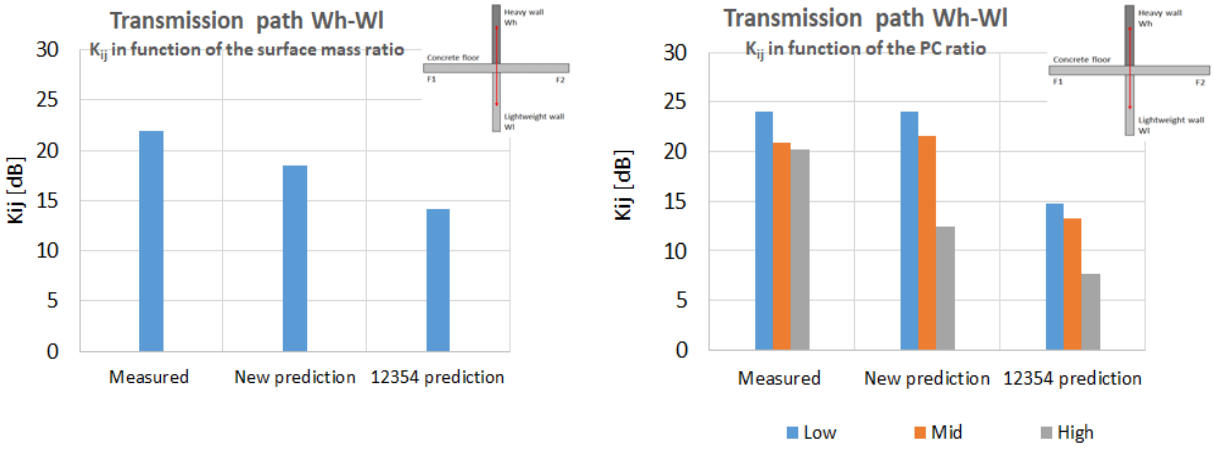

(a) (b)

Figure 13: Path Wh-Wl: Comparison between the measured results, the new prediction results and the prediction results obtained according to the annex J of the standard 12354. (a) for K_{ij} expressed in terms of the surface mass ratio, (b) for K_{ij} expressed in terms of PC ratio.

For the path Wh-Wl (Figure 13a and 13b), the improvement with the new prediction is significant. Particularly, the results obtained with the new prediction are very close to the expected values for the estimation of the $K_{ij,mid}$ and $K_{ij,low}$ expressed in terms of the PC ratio.

The results for the path F1-Wh (Figures 14) are somewhat disappointing. A degradation of the prediction is observed but it is attributed to the fact that the K_{ij} values of the cross-junction and the T-junction given by the standard 12354 are underestimated. Indeed, a previous testing program carried out on simple cross-junctions and T-junctions showed that the 12354-1 prediction values were ± 5 dB lower than the measured values [16].

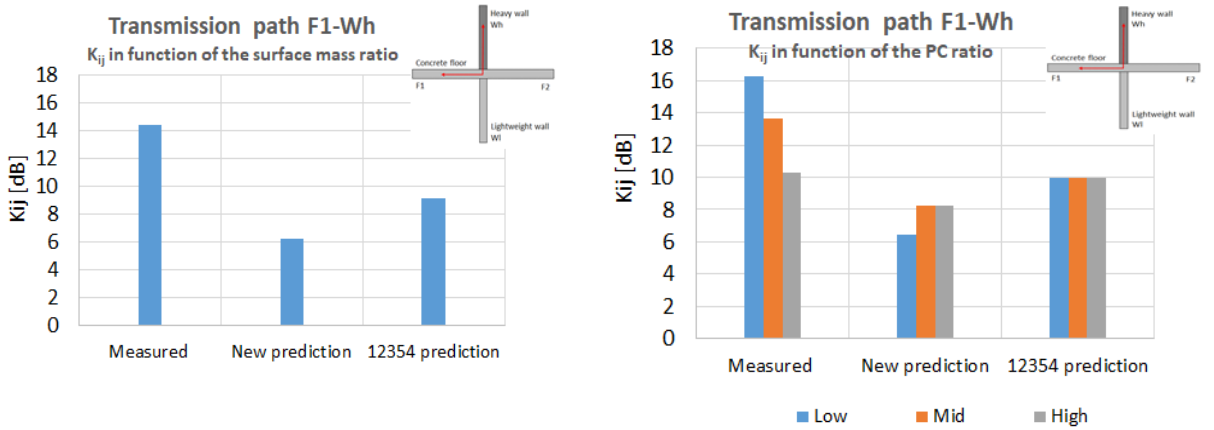

(a) (b)

Figure 14: Path F1-Wh: Comparison between the measured results, the new prediction results and the prediction results obtained according to the annex J of the standard 12354 (Wmean prediction). (a) for K_{ij} expressed in terms of the surface mass ratio, (b) for K_{ij} expressed in terms of PC ratio.

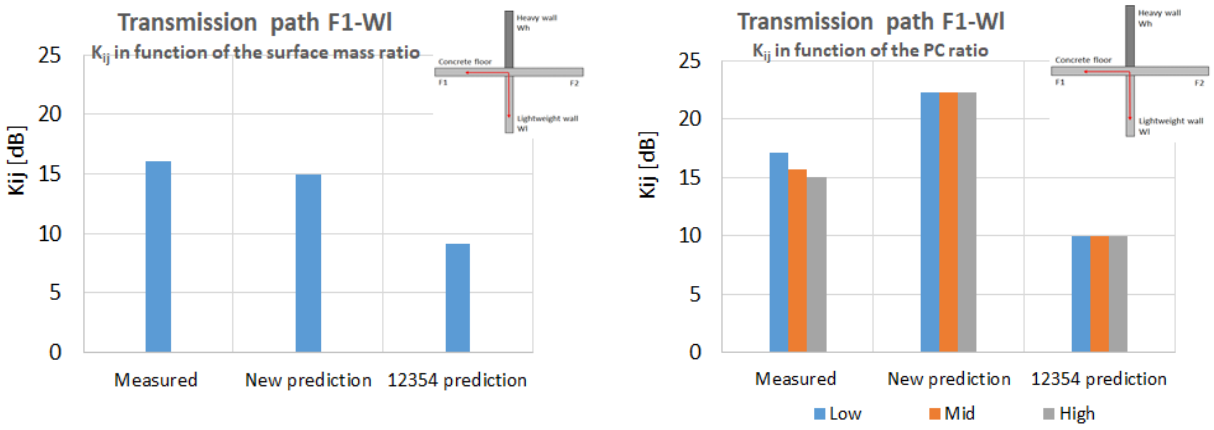

(a) (b)

Figure 15: Path F1-Wl: Comparison between the measured results, the new prediction results and the prediction results obtained according to the annex J of the standard 12354. (a) for K_{ij} expressed in terms of the surface mass ratio, (b) for K_{ij} expressed in terms of PC ratio.

For the path F1-Wl, a best estimation is obtained with the new prediction for the K_{ij} expressed in terms of the surface mass ratio (Figure 15a). However, an excessive overestimation is observed for the estimation of the K_{ij} expressed in terms of the PC ratio which is not on the safe side as preferred for the predictions (Figure 15b).

7 Conclusion

This article proposes new prediction formulas to evaluate the vibration reduction index K_{ij} for rigid mixed cross-junctions. These formulas which were derivated from a large number of numerical simulations are relatively simple. They are based on the weighting of K_{ij} of simple rigid cross- and T- junctions. The weight factor p is expressed by the ratio of the surface masses or the PC ratio according to both approaches that recently appeared in the standard ISO 12354-1.

The numerical simulations have shown an obvious improvement of the new prediction compared to the proposition which idealizes the junction by averaging the surface masses of the two different coplanar walls (annex J of the standard 12354). The calculations errors obtained with this idealization can be very high and increases significantly when the contrast between the surface masses increases while the new prediction results remain very close to the expected results.

The comparison between measurement and prediction results shows, in general, the best agreement if the weight factor p is used. An excessive overestimation of the vibration reduction index is however observed for a few cases, which is not on the safe side as preferred for predictions.

Acknowledgements

The authors wish to acknowledge the financial assistance of the Federal Public Service Economy of Belgium.

References

[1] ISO 10848-1 to 4 (2017). Acoustics - Laboratory and field measurement of flanking transmission for airborne, impact and building service equipment sound between adjoining rooms;

[2] ISO 12354-1 (2017) Building Acoustics — Estimation of acoustic performance of buildings from the performance of elements — Part 1: Airborne sound insulation between rooms;
[3] Hopkins C., Crispin C., Poblet-Puig J., Guigou-Carter C., Regression curves for vibration transmission across junctions of heavyweight walls and floors based on finite element methods and wave theory, *Applied Acoustics* 113 (2016) 7-21.
[4] Crispin C., De Geetere L., Ingelaere B., Extensions of EN 12354 vibration reduction index expressions by means of FEM calculations, *Proceedings of Internoise*, Melbourne, Australia, 16-19 November(2014).
[5] Crispin C., Mertens C., Dijckmans A., Detailed analysis of measurement results of flanking transmission across a junction composed of double walls carried out on a half scaled test bench, *Proceedings of* ICSV24, 23-27 July 2017, London.
[6] Kling C., Miniaturising a wall test facility, *Journal of Building Acoustics*, Vol. 14, N°4, 2007, 243-266.
[7] Wittstock V., Schmelzer M., Kling C., On the use of scaled models in building acoustics, *Proceedings of Euronoise*, Paris, France, 29 June-4 July(2008).
[8] Crispin C., Mertens C., Dijckmans A. Integrating lightweight concepts in acoustical standardization. BBRI Technical Report, DIVA2018/CCR001 (2018)
[9] Dijckmans A. , "Structure-borne sound transmission across junctions of finite single and double walls", *Proceedings of Inter-Noise 2015,* San Francisco, USA, (2015)
[10] Gerretsen, E., "Calculation of sound transmission between dwellings by partitions and flanking structures", Applied Acoustics 12 (1979), 413-433.
[11] C. Hopkins, Sound insulation, Butterworth-Heineman, Amsterdam e.d., 2007
[12] Poblet-Puig J., Guigou-Carter C., Amplified catalogue of vibration reduction index formulas for junction based on numerical simulations, *Proceedings of Internoise*, Hamburg, Germany, 21-24 August, (2016).
[13] Dijckmans A., Vibration transmission across junctions of double walls using the wave approach and statistical energy analysis, *Acta Acustica united with Acustica*, Vol. 102 (2016) 488-502.
[14] Dijckmans A. Wave based modelling of vibration transmission across junctions composed of rectangular single and double walls, *Acta Acustica united with Acustica*, Vol. 102 (2016) 1011-1026.
[15] Poblet-Puig J., Guigou-Carter C., Using spectral finite elements for parametric analysis of vibration reduction index of heavy junctions oriented to flanking transmissions and EN-12354 prediction method, *Applied Acoustics* 99 (2015), 8-23.
[16] BBRI, Integrating lightweight concepts in acoustical standardization (A-Light). Research projet (2016-2018)